Transverse Cooling or Heating of Channeled Ions by Electron Capture and Loss

W. Assmann,[1] H. Huber,[1] S. A. Karamian,[2] F. Grüner,[1] H. D. Mieskes,[1] J. U. Andersen,[3] M. Posselt,[4] and B. Schmidt[4]
[1]*Sektion Physik, LMU München, D-85748 Garching, Germany*
[2]*FLNR JINR, 141980 Dubna, Russian Federation*
[3]*ACAP, Institute of Physics and Astronomy, Aarhus University, Aarhus C, Denmark DK 8000*
[4]*Forschungszentrum Rossendorf, D-01314 Dresden, Germany*
(Received 8 February 1999)

We have measured the angular distribution of energetic heavy ions after passage through a Si crystal for an incident beam with an isotropic angular distribution over angles much larger than the critical angle for channeling. Strong redistribution of the flux has been observed, in some cases an enhancement along channeling directions, and in other cases a reduction. The phenomenon is not predicted by channeling theory and cannot be reproduced by computer simulations. We propose a new mechanism: cooling or heating of the transverse motion of channeled ions due to repeated capture and loss of electrons. The cooling effect is analogous to Sisyphus cooling of very cold, trapped atoms in a strong laser field.

PACS numbers: 34.70.+e, 34.20.Cf, 61.85.+p

Energetic charged particles entering a crystal nearly parallel to an axis or a plane become channeled; their motion is guided by correlated collisions with atoms on atomic rows or in atomic planes [1,2]. For incidence outside a critical angle, the particles move nearly as in a random medium. During penetration of a thick crystal, there will be transitions due to multiple scattering. Scattering from the channeled to the random beam (dechanneling) and from the random to the channeled beam (feeding-in) are both suppressed by the channeling effect, and according to a general principle of reversibility, the two transition rates are equal if energy loss can be neglected [2,3]. Hence, an initially isotropic angular distribution is expected to be stable under transmission through a crystal. A small deviation from reversibility, due, for example, to energy loss, would be easy to detect under these conditions, and this was the purpose of our experiment. Although the symmetry required for stability of an isotropic angular distribution is a symmetry in momentum space of the scattering events [3], it is closely connected to time reversibility of trajectories and the equivalence of channeling and blocking [2,4].

In this Letter, we present experimental evidence for a redistribution of particle flux from an initially isotropic angular distribution after transmission through thin single crystals. We have observed an increase as well as a decrease of the particle flux in the direction of axes or planes, depending on the experimental conditions. Such behavior was not predicted by existing theory and could not be reproduced by computer simulations. The effect is not related to the well known flux peaking of channeled particles which is flux enhancement in space, not in angle. We propose a new mechanism to be responsible for the observed effects, related to the irreversibility of charge exchange processes along an ion trajectory.

Most previous studies of the development of a charged particle flux in single crystals have used collimated beams in order to prepare well defined initial conditions. Channeling or blocking behavior has been observed after transmission through monocrystalline foils of appropriate thickness, depending on the incidence angle of the ions [5–7]. However, reversibility of multiple scattering is not tested under these conditions. In other experiments, α particles from a radioactive source have been used to generate an isotropic ion distribution and channeling patterns have been measured after transmission of thin crystals by track detectors or photographic plates [8,9]. But, because of the energy selection by an absorber in front of the crystal or by the detector itself, no quantitative comparison has been possible between channeled and random particles. The reversibility of multiple scattering has been confirmed in experiments at very high energies where both energy loss and charge exchange can be neglected [10].

In our earlier experiments, an angular distribution of recoil atoms was created inside a Si crystal by scattering energetic, heavy projectiles [11,12]. We selected different depths of origin by an appropriate choice of the incidence or exit energy and observed a transition, with increasing path length in Si, from a suppression to an enhancement of the intensity in channeling direction. However, the energy selection may have favored channeled over random particles due to the difference in energy loss. Therefore, we chose a new scattering geometry for the present measurements.

The experimental setup consists of a high vacuum chamber with a 5-axis sample positioning system and a large-area position sensitive gas ionization detector, which can be positioned at different scattering angles [13]. A beam of 210 MeV I or 230 MeV Au ions was incident on a scattering target and the recoils (or scattered ions) were detected after transmission through a thin Si crystal (see Fig. 1). The scattering targets consisted of C, Al, Cu, or Au with thicknesses of 40 to 180 $\mu g/cm^2$. Experiments were performed with (001) Si crystals of 2.9 to 8.7 μm thickness, prepared by electrochemical etching with an

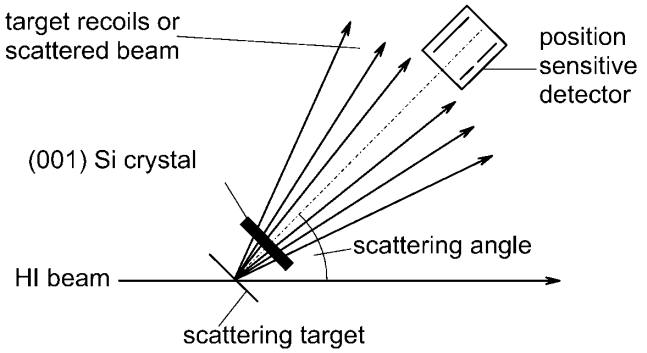

FIG. 1. Schematic of the experimental geometry.

ion-implanted etch stop [14]. The direct beam could not hit the Si crystal after the scattering target and, therefore, radiation induced damage or dimpling was avoided. In order to have the (amorphous) native oxide layers removed, the Si foils were etched by a short HF dip immediately before being mounted in vacuum. The recoil energy was changed by selection of two different scattering angles (37.6° or 50.2°) and in some measurements by an Al absorber foil in front of the Si crystal. The elastic recoil cross section varied at most by 30% within the angular acceptance of our detector (±2.2°). Thus the initial flux of scattered ions could, to first approximation, be assumed to be uniformly distributed over the measured angular range.

Figure 2 shows angular distributions of scattered ions or recoils, after transmission through an 8.7 or 2.9 μm thick (001) Si foil. Recoil atoms and scattered projectiles were separated in the detector but no selection on energy was applied. The particle density is represented by the pixel gray level with darker gray indicating higher density. Flux enhancement is obvious for C recoils along the ⟨100⟩ axis and along the {100} and {110} planes. A surprising feature is seen for Cu recoils, which exhibit enhanced and reduced flux simultaneously. This behavior remains to some extent for I ions, whereas Au ions show a strong flux reduction along the crystal axis and planes. Circular averaging around the axis was used to obtain the ion yield as a function of the angle to the axis, plotted in Fig. 2 together with the corresponding flux patterns. This procedure eliminates planar effects as well as the asymmetry due to the scattering angular distribution. Flux patterns with energy selection of particles (not shown) indicate that channeled ions have less energy loss than random ions, but the difference in exit energy is only about 15%.

In this paper we shall discuss mainly axial effects, and Table I summarizes the results of our experiments for different ions along a ⟨100⟩ axis in Si. We have included in Table I two results of experiments with He ions, where a nuclear track detector was used in a setup similar to that described in [9]. The final energy, E_f, after transmission through the Si foil was calculated with TRIM for random energy loss. The measured half angle of the flux peak (or dip in the case of Au and I) is compared with the Lindhard critical angle [2] for channeling in the last two columns. The small value of $\psi_{1/2}^{\mathrm{exp}}$ for Cu (and I) should be noted which is limited by the experimental resolution.

In order to understand the physical reason for the observed flux redistribution it was important to know if it could be reproduced by computer simulations. We used the binary collision code CRYSTAL-TRIM [15] which takes into account the nuclear energy loss and angular scattering in the universal-potential approximation, the electronic

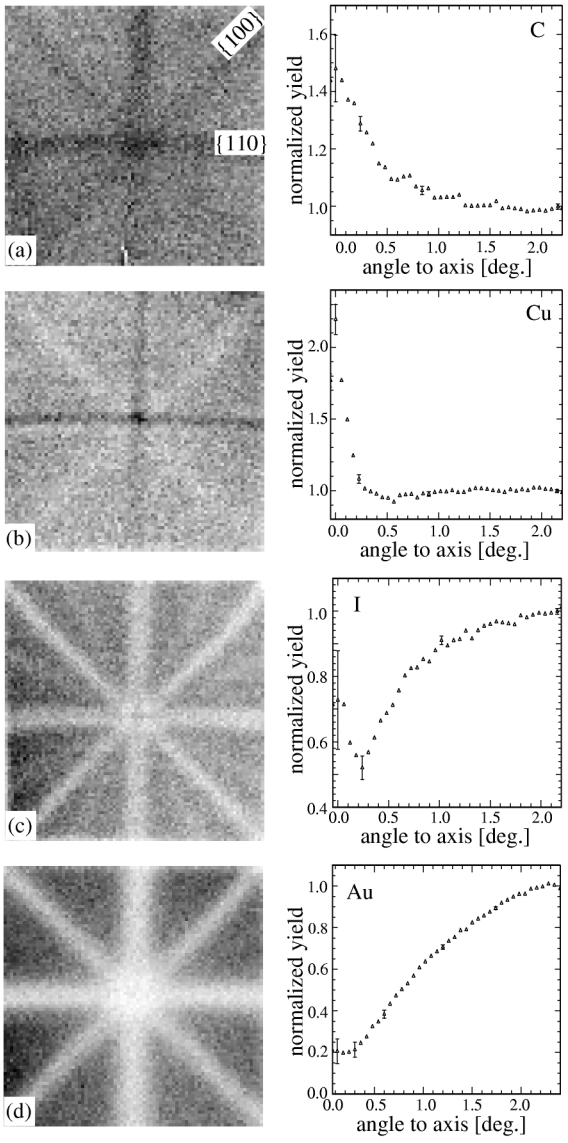

FIG. 2. Flux distributions of heavy ions after transmission of (001) Si foils, and corresponding circular averages around the ⟨100⟩ axis at varying polar angle: (a) C recoils at 18 MeV after 8.7 μm Si; (b) Cu recoils at 46 MeV after 8.7 μm Si; (c) scattered I ions at 121 MeV after 2.9 μm Si; and (d) scattered Au ions at 92 MeV after 2.9 μm Si. The angular range of the patterns is ±2.2° around the ⟨100⟩ axis in the center. Planar directions are indicated in (a).

TABLE I. Results of flux distribution measurements after transmission of (001) Si foils. E_i and E_f are the entrance and exit energies of the ions for random energy loss. t indicates the foil thickness and χ_a the flux in direction of the $\langle 100 \rangle$ axis. The measured half angle $\psi_{1/2}^{\text{exp}}$ of the peak (or dip) is compared with the Lindhard angle ψ_1 for axial channeling at E_f.

Ion	E_i (MeV)	E_f (MeV)	t (μm)	χ_a	$\psi_{1/2}^{\text{exp}}$ (deg)	ψ_1 (deg)
Au	130	92	2.9	0.18 ± 0.02	0.95 ± 0.05	0.46
I	157	121	2.9	0.52 ± 0.04[a]	0.74 ± 0.05[a]	0.33
Cu	113	90	2.9	1.12 ± 0.05	···	0.28
Cu	113	46	8.7	2.19 ± 0.11	0.12 ± 0.02	0.39
Al	74	52	8.7	1.60 ± 0.10	0.22 ± 0.02	0.25
Al	48	23	8.7	2.20 ± 0.05	0.22 ± 0.02	0.37
C	42	36	8.7	1.12 ± 0.05	···	0.20
C	26	18	8.7	1.48 ± 0.12	0.30 ± 0.02	0.29
He	4.5	3.1	8.7	1.18 ± 0.05[b]	0.50 ± 0.10[b]	0.40
He	3.5	1.7	8.7	1.32 ± 0.05[b]	0.65 ± 0.10[b]	0.54

[a]Value at 0.22° with corresponding half angle, flux peak at 0° with 0.12° half angle.
[b]Measured with nuclear track detector.

energy loss (either nonlocal or impact parameter dependent), and multiple scattering on electrons. A Gaussian distribution of the atomic displacements simulated the thermal vibrations (Debye model). Most of the calculations were performed for transmission of 48 MeV Al ions through an 8.7 μm thick (001) Si crystal. The starting points of the particles were randomly distributed over the area of a Si elementary cell (5.43 × 5.43 Å^2) with polar angles between 0° and 4°. This restriction was necessary to avoid excessively long computing times, but a normalization procedure had to be applied to compensate for the broadening of the angular distribution. The calculated angular distribution of the particles after transmission through a 8.7 μm Si did not exhibit significant deviations from a random distribution. The results were in agreement with calculations using the LAROSE code [16]. Thus, state-of-the-art simulation programs which take into account all energy loss effects do not reproduce our experimental observation.

It is perhaps not surprising that energy loss has little effect on the angular distribution of transmitted ions. If the stopping were the same for channeled and random ions (nonlocal stopping), the angular distribution would be completely unaffected. The damping term representing energy loss in descriptions of multiple scattering as diffusion in transverse energy [2] then exactly compensates for the increase of the Lindhard angle, $\psi_1 \propto E^{-1/2}$. As mentioned above, the lower stopping for channeled ions leads to a slightly higher average energy for ions exiting the crystal parallel to an axis or a plane, and this could lead to a distortion of the isotropic distribution. But the simulations have demonstrated that this distortion is very small.

We suggest that the observed effects are instead caused by charge exchange. A swift, heavy ion has an average net charge $Z_1^* e$ given approximately by $Z_1^* \simeq Z_1^{1/3} v/v_0$, where Z_1 is the atomic number and v the velocity of the ion and $v_0 = e^2/\hbar$ is the Bohr velocity [17]. The ion charge is in dynamical equilibrium, fluctuating rapidly due to capture and loss of electrons. As illustrated in Fig. 3, a capture and loss cycle changes the transverse energy of an ion. Considering an ion as a point charge its transverse energy may be written as $E_\perp = p_\perp^2/2M_1 + Z_1^* U(r)$ where $U(r)$ is the potential for a proton. The point-charge approximation is not always very accurate but, qualitatively, this does not affect the following argumentation. If an electron is captured at distance r_c and lost at a larger distance r_l, the ion experiences a net loss in transverse energy, $\Delta E_\perp = U(r_l) - U(r_c)$, as indicated in the figure. The electron is carried away from the atomic row, up a potential hill for the electron, and then lost. This effect is analogous to Sisyphus cooling of very cold, trapped atoms in strong laser fields [18]. If, on the average, $r_l > r_c$, capture and loss will lead to an increase in the density of ions at small $E_\perp$ and therefore to an enhancement of the flux of ions exiting the crystal nearly parallel to the axis.

An indication in favor of this explanation of the observed anisotropies of the ion flux is obtained from the energy dependence for He and C beams, seen in Table I. The anisotropy is much smaller at the higher energies where the probability for carrying even a single electron is small [19]. But a more severe test is explanation of the reversal of cooling to heating, illustrated in Fig. 2. The impact parameter dependence of capture and loss can be estimated on the basis of the simple concepts introduced by Bohr and Lindhard [17], which account fairly well for measured capture cross sections for highly charged ions [20]. A characteristic impact parameter R_l for electron

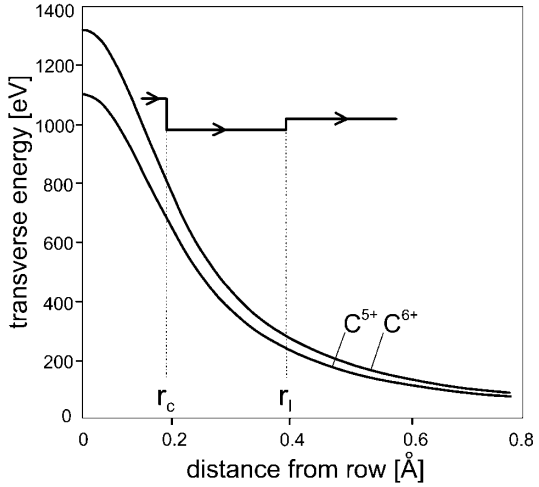

FIG. 3. Atomic-row potentials for C^{5+} and C^{6+} ions, in the point-charge approximation. The horizontal line indicates the transverse energy of a C^{6+} ion moving along an atomic row, capturing an electron at r_c and losing it at r_l.

TABLE II. Characteristic distances in Å for capture of Si L-shell electrons and for electron loss.

Ion	E (MeV/u)	Z_1^{*} [a]	R_{2s} [b]	R_{2p} [b]	R' [c]	R_l [d]
C	1.5	5.5	0.13	0.22	0.10	0.17
Cu	1.0	18	0.23	0.39	0.48	0.23
I	1.0	27	0.28	0.48	0.72	0.23
Au	0.5	28	0.29	0.49	1.50	0.33

[a]Mean charge after transmission through a carbon foil [19].
[b]From Eq. (1), equivalent to Eq. (4.3) in [17].
[c]From Eq. (2), equivalent to Eq. (4.4) in [17].
[d]From the Thomson cross section [Eq. (4.1) in [17]], corrected for screening with the Lindhard standard potential [2]. The minimum energy transfer for ionization was assumed to be $\sim\frac{1}{2}mv^2$ except for C where the K-shell binding energy was used.

loss can be obtained from the classical Thomson cross section, with a correction for screening of the nuclear Si potential. For capture there are two important distances. The release radius R is defined as the distance at which the Coulomb force from the ion equals the binding force in the atom, and it is given approximately by

$$R = Z_1^{*1/2} n^2 (Z_2 - s)^{-3/2} a_0 \qquad (1)$$

for an electron with main quantum number n in an atom with atomic number Z_2. Here a_0 is the Bohr radius and s is the Slater screening correction ($s = 2.4$ for $2s$ electrons and 5.8 for $2p$ electrons) [21]. The electron is released with very small energy in the laboratory frame and therefore has a kinetic energy $\sim\frac{1}{2}mv^2$ in the ion frame. It will be captured if this energy is smaller than its potential energy in the ion field, i.e., for $R < R'$, where

$$R' = 2Z_1^{*}\left(\frac{v_0}{v}\right)^2 a_0 . \qquad (2)$$

For $R > R'$ there can be capture due to delayed release, but with smaller probability. The characteristic distances for capture from the Si L shell are given in Table II for the four cases illustrated in Fig. 2. There is little capture from the M shell because $R > R'$, except perhaps for Au. The characteristic distances for capture and loss in a single collision with a Si atom give estimates of the corresponding distances r_c and r_l from an atomic row. Since the smaller of the release and capture radii determines the capture distance, the values for C in Table II predict a cooling effect, as observed in Fig. 2. For Cu, I, and Au the relative magnitude of the two radii is reversed and a heating effect is predicted. Cu is experimentally observed to be an intermediate case, with cooling for well channeled ions and heating for poorly channeled ions and for channeling along weaker planes. This could be due to electron loss in collisions with valence electrons at large impact parameters, where capture decreases very rapidly.

In conclusion, our experiments have shed new light on the basic symmetry of ion scattering in crystals. Notwithstanding the cursory nature of the theoretical estimates, the qualitative agreement between predictions and experiments provides strong evidence for an explanation of the observed flux redistribution in terms of transverse cooling or heating by capture and loss of electrons. The prediction for C ions in Table II that electron capture decreases more rapidly with impact parameter than electron loss is supported by measurements in Ref. [22] of charge state distributions for O ions channeled through a thin gold crystal, and the prediction of the opposite behavior for I ions is supported by similar measurements [23].

[1] D. S. Gemmell, Rev. Mod. Phys. **46**, 129 (1974).
[2] J. Lindhard, Mat. Fys. Medd. K. Dan. Vidensk. Selsk. **34**, No. 14 (1965).
[3] J. Lindhard and V. Nielsen, Mat. Fys. Medd. K. Dan. Vidensk. Selsk. **38**, No. 9 (1971).
[4] E. Bøgh and J. L. Whitton, Phys. Rev. Lett. **19**, 553 (1967).
[5] G. Della Mea *et al.*, Nucl. Instrum. Methods **132**, 163 (1976).
[6] G. Dearnaley *et al.*, Philos. Mag. **18**, 985 (1968).
[7] R. E. Holland and D. S. Gemmell, Phys. Rev. **173**, 344 (1968).
[8] Y. Quéré and H. Couve, J. Appl. Phys. **39**, 4012 (1968).
[9] V. V. Skvortsov and I. P. Bogdanovskaya, Sov. Phys. JETP Lett. **11**, 1 (1970).
[10] J. S. Forster, in *Relativistic Channeling*, edited by R. A. Carrigan, Jr. and J. A. Ellison (Plenum, New York, 1987).
[11] S. A. Karamian, Nucl. Instrum. Methods Phys. Res., Sect. B **51**, 354 (1990).
[12] W. Assmann *et al.*, Nucl. Instrum. Methods Phys. Res., Sect. B **118**, 242 (1996).
[13] W. Assmann *et al.*, Nucl. Instrum. Methods Phys. Res., Sect. B **85**, 726 (1994).
[14] B. Schmidt, J. von Borany, U. Todt, and A. Erlebach, Sens. Actuators A **41–42**, 689 (1994).
[15] M. Posselt, Radiat. Eff. Defects Solids **130/131**, 87 (1994).
[16] J. Barrett (private communication).
[17] N. Bohr and J. Lindhard, Dan. Mat. Fys. Medd. **28**, No. 7 (1954).
[18] A. Aspect, J. Dalibard, A. Heidmann, C. Solomon, and C. Cohen-Tannoudji, Phys. Rev. Lett. **57**, 1688 (1986).
[19] K. Shima *et al.*, At. Data Nucl. Data Tables **51**, 174 (1992).
[20] H. Knudsen, H. K. Haugen, and P. Hvelplund, Phys. Rev. A **23**, 597 (1981).
[21] J. C. Slater, *Quantum Theory of Atomic Structure* (McGraw-Hill, New York, 1960), Vol. I, p. 369.
[22] S. Datz, F. W. Martin, C. D. Moak, B. R. Appelton, and L. B. Bridwell, Radiat. Eff. **12**, 163 (1972).
[23] H. O. Lutz, S. Datz, C. D. Moak, and T. S. Noggle, Phys. Lett. **33A**, 309 (1970).